The small focus diameter of fiber lasers offer a number of advantages during laser welding:

- High power density at the workpiece
- Reduced heat input
- Reduced heat-affected zone
- Reduced cycle time
- The volume of intermetallics may also be reduced to acceptable limits.

Fiber laser welding can be carried out using a single mode fiber laser with average power exceeding 2kW or a multi-mode fiber lasers with laser powers excess of 17kW. Multi-mode fiber lasers normally comprise several single mode fiber lasers, which are coupled into one fiber with reduced beam quality. However, the beam quality is still good enough to use small core diameter fibres, thus enabling very high power density at the workpiece.

From an applications perspective, both single and multi-mode fiber lasers have their advantages and disadvantages when welding dissimilar materials. This paper highlights welding results achieved for a range of dissimilar material combinations, using a 1kW multi-mode fiber laser.

Experimental work

A multi-mode 1kW fiber laser (1000FL) with a maximum average output power of 1000W was used in this study. Beam product parameters (BPP) of this laser are ≤ 4 mm·mrad. The beam from the laser was transmitted in 100µm diameter fiber which terminated in right-angled output housing fitted with recoll and focusing optics. The calculated spot size at the workpiece was 150µm.

Laser welding experiments were performed on different metal combinations:

- Titanium alloy – aluminium alloy
- Copper – 304 stainless steel
- Copper – aluminium alloy

The most important thermo-physical properties of the corresponding metals are shown in Table 2. Although these values refer to pure metals and some properties are temperature dependent, the data provided is a basic reference for assessing weldability and deriving the welding strategy.

Metals	Coefficient of thermal expansion $X10^{-6}$ K^{-1}	Latent heat fusion Jg^{-1}	Specific heat JK^{-1} kg^{-1}	Thermal conductivity Wm^{-1} K^{-1}	Melting point °C	Boiling point °C	Density gcm^{-3}
Aluminium	23.5 @ 0-100C	388	900 @25C	237@ 0-100C	660	2467	2.7
Copper	17.0 @ 0-100C	205	388 @25C	401@ 0-100C	1083	2870	8.96
Iron	12.1 @ 0-100C	272	444 @25C	81@ 0-100C	1535	2750	2.87
Titanium	8.9 @ 0-100C	365	523 @25C	21.9@ 0-100C	1660	3287	4.5

Table 2: Thermophysical properties of some metals

Parameters and welding speeds were adjusted to produce welds with consistent topbead and underbead, minimal spatter and undercut. Gas shielding for the weld topbead was supplied via a 10mm diameter pipe (Figure 3). In all cases, argon (10l/min) was used for shielding.

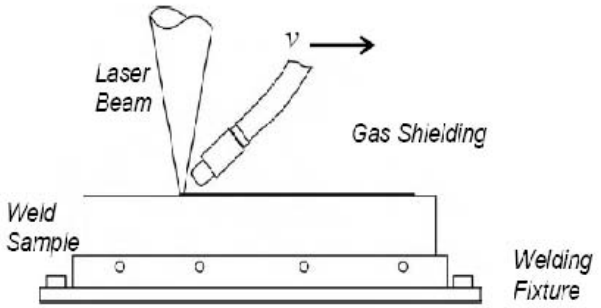

Figure 3: Gas shielding arrangement

Results and Discussion

Titanium/Aluminium Alloy

Recently, demand for dissimilar metal joints of titanium to aluminium alloy has risen in industry, especially in the transportation vehicle industry. However, it is well known that fusion welding of titanium to aluminium alloy is difficult because of the brittle intermetallic compound that is generated at the joint interface.

Figure 4 shows a photo-macrograph of the weld between Ti alloy and Al. The weld was very wide but the penetration into the lower aluminium sheet was very shallow.

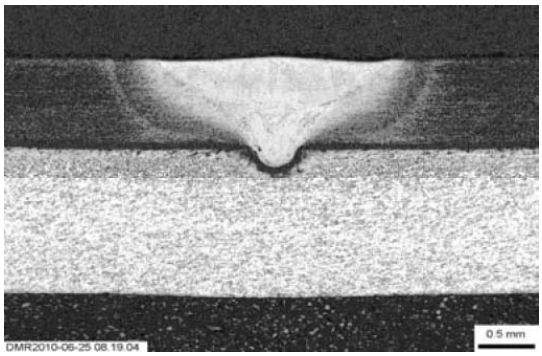

Figure 4: Photo-macrograph of the weld between Ti alloy and Al alloy. The specimen was etched with Kellers' reagent.

Figure 5 shows the bottom part of the weld where the two sheets were jointed. At the root of the weld there was a zone measuring approximately 150µm wide where aluminium had melted but not mixed with the remainder of the weld pool. The interface between the mixed molten metal and the melted Al was 'fluffy' with a lot of swirls where there was variable mixing of the melted sheets.

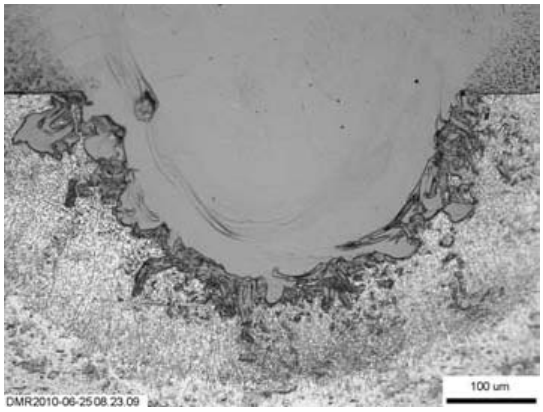

Figure 5: The root of the weld between Ti alloy and Al alloy. The specimen was etched with Kellers' reagent

Figure 6 shows an SEM micrograph with the location of EDX analyses. The Ti sheet was consistent with the Ti--6Al-4V alloy and the Al contained a little Fe, Mn and Mg, consistent with a 3000 (Al-Mn) series Al alloy.

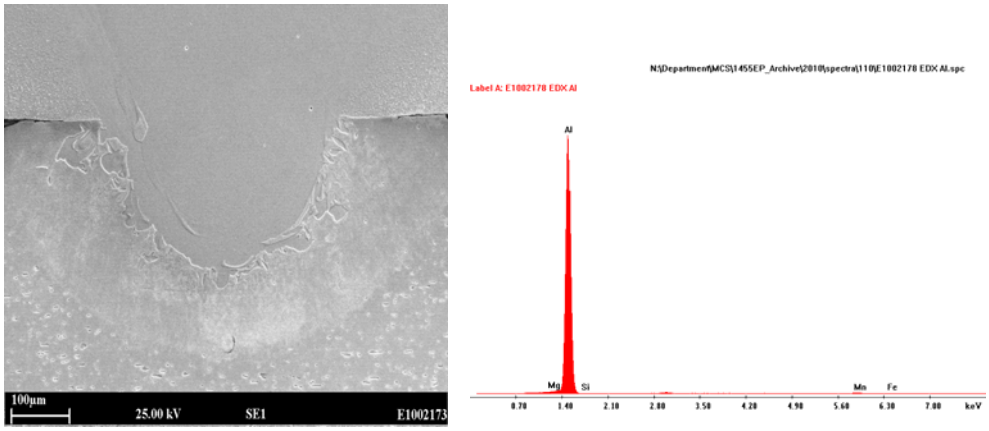

Figure 6: SEM micrograph of the root of the Ti-Al weld and EDX analysis spectra

A few, isolated, micro pores can be observed in Figures 4-6. The compositions in locations 1, 3 and 5 were similar, consisting mainly of the Ti alloy with only a small dilution with Al.

Stainless Steel/Copper

In the field of power generation and transmission, cryogenics, electrical and electronics, copper–steel combinations are often used due to their high electrical conductivity and stiffness. However, the high thermal conductivity of copper tends to rapidly dissipate heat away from the weld, leading to difficulties in reaching the melting temperature.

The major problem in welding copper to steel is hot cracking in the heat-affected zone of steel due to copper melting and penetrating into the grain boundaries of solid steel. Figure 7 shows the weld of stainless steel to copper. This was a fully penetrated weld. The bottom part of the weld had an inhomogeneous structure but the top part was relatively uniform.

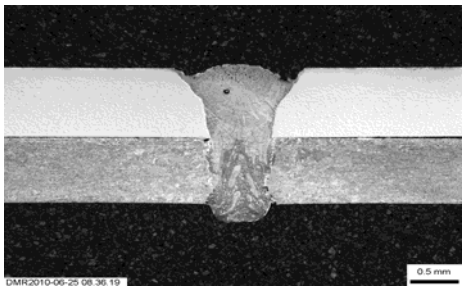

Figure 7: Photomacrograph of the weld between 304 stainless steel and Cu etched electrolytically in 20% H_2SO_4 + 0.1 g/l NH_4CNS and by immersion in ferric chloride

Figure 8 shows an SEM image of the weld and EDX analysis that was conducted for the sheets. It was confirmed that the copper sheet was pure Cu. The composition of the 304 stainless steel sheet was also confirmed.

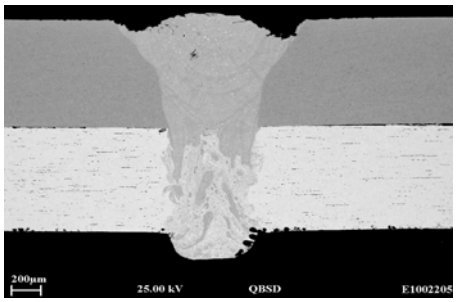

Figure 8.a SEM micrograph of the profile of the weld between stainless steel in the as-polished condition and Cu

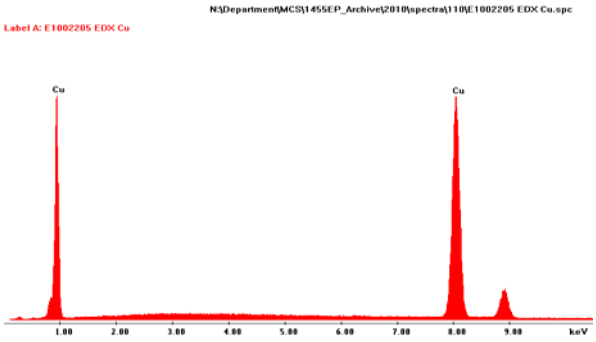

Figure 8.b EDX spectrum from the Cu sheet

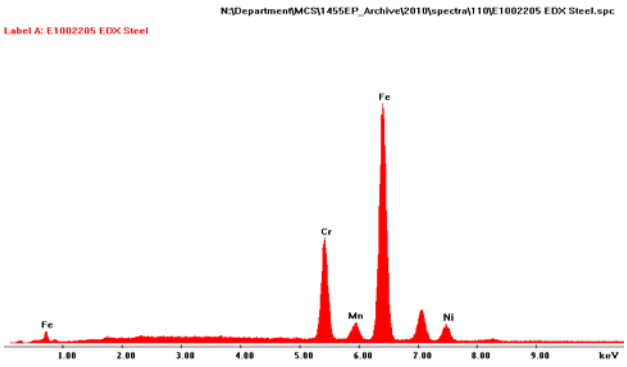

Figure 8.c EDX spectrum from the stainless steel sheet

At higher magnification, Figure 9 shows a small region of solidification cracking in the centre of the weld surrounded by many steel-rich spherical particles in a copper rich matrix.

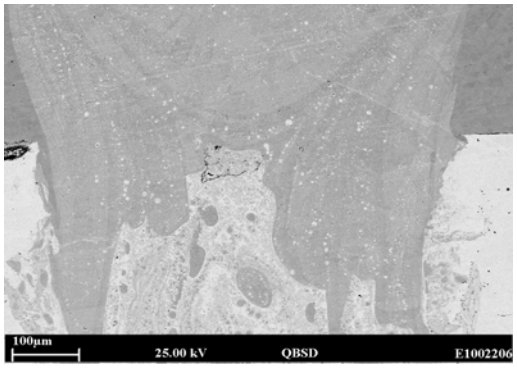

Figure 9.a: A low magnification SEM micrograph of solidification cracking in the centre of the weld between 304 stainless steel and Cu in the as-polished condition.

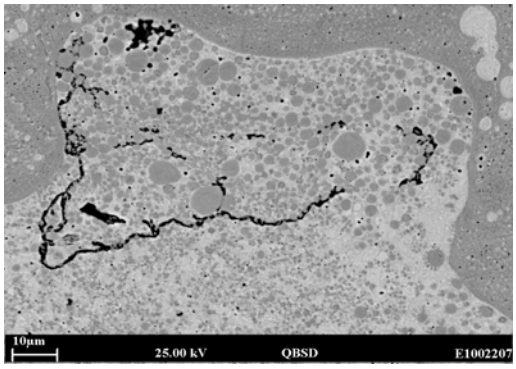

Figure 9.b: A high magnification SEM micrograph of solidification cracking in the centre of the weld between 304 stainless steel and Cu in the as-polished condition.

Aluminium/Copper

Joints between aluminum and copper are often required in electronic and automotive market sectors. The battery for hybrid cars is mainly constructed from a combination of aluminium alloys (3003 series, AL-Mn alloy) and pure copper. Joining these materials pose particular challenges. The battery has to operate safely and reliably for the whole of the life cycle stipulated by the manufacturer, and that's at least ten years.

Figures 10 and 11 show the weld between Al alloy and Cu and an SEM micrograph is shown in Figure 12. It can be seen that the penetration into Cu was low and there were many cracks in the lower part of the weld.

Figure 13 shows detail of the crack morphology and the locations for EDX analyses. The cracks were brittle in character and all stopped at the interface between the weld and the Cu parent metal. The analyses suggest (Figure 13b) a number of phases are present i.e. very close to $CuAl_2$.

Another similar analysis (figure 14) was carried out at the edge of the weld near the interface between the sheets, where a long interfacial crack extended into the lower part of the weld. This crack was also brittle in character, similar to the cracks in other locations of the weld. However, there were no cracks observed in the upper part of the weld, where dilution of the Al by Cu was low.

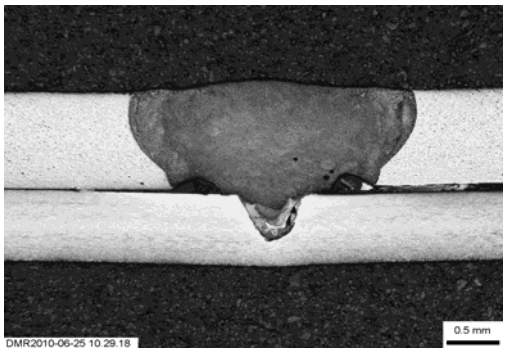

Figure 10: Photomacrograph of the weld between Al alloy and Cu, etched in Kellers' reagent + ferric chloride

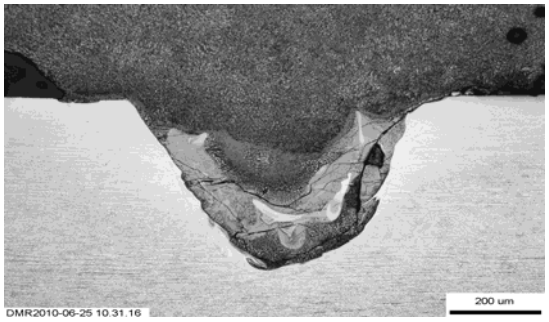

Figure 11: The root of the weld between Al alloy and Cu, etched in Kellers' reagent + ferric chloride

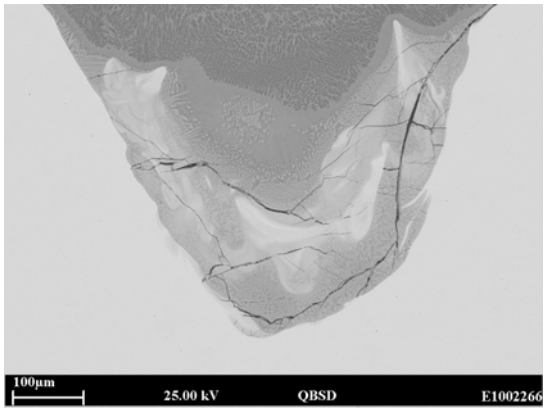

Figure 12: SEM micrograph of the root of the weld between Al alloy and Cu

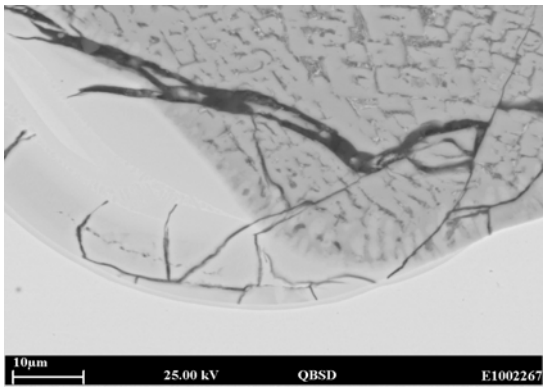

Figure 13a: SEM micrograph of the interface between the weld and Cu sheet in the weld between Al alloy and Cu

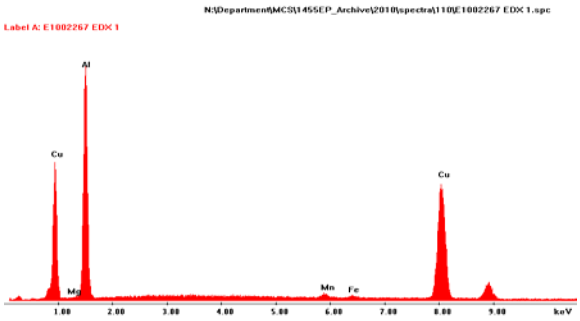

Figure 13b: EDX spectra near the bottom of the weld

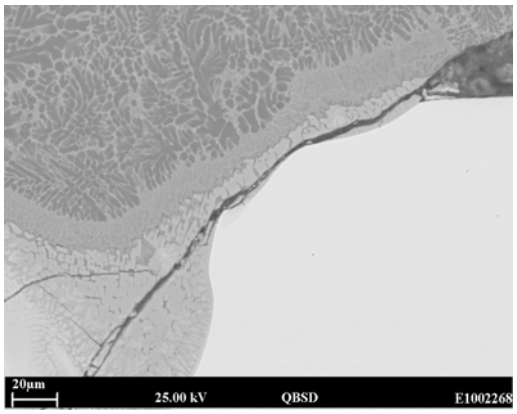

Figure 14a: SEM micrograph of the interface between the weld and Cu sheet in the weld between Al alloy and Cu.

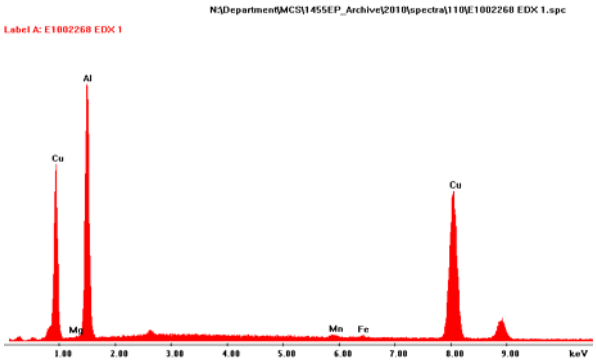

Figure 14b: EDX spectra near the bottom of the weld.

Summary

The presence of dissimilar materials highlighted differences in the behaviour of laser welding, compared to other fusion welding processes such as arc welding. Thus, mixing in the weld pools was relatively poor and there were usually two distinct regions in each weld cross section, corresponding to where the pool was surrounded by each sheet.

Where there were large differences in melting point between the sheets, e.g. Ti and Al, there was a region, within the lower melting point sheet, which had melted but not mixed with the main weld pool.

Few problems would were anticipated with joints between dissimilar copper alloys, and this generally proved to be the case. Although austenitic stainless steel and copper alloys were characterised by a mixture of copper and iron-rich phases, these welds were mostly sound.

However, the joints with the aluminium alloy sheets contained significant cracking. Both welds to copper and stainless steel-plated copper contained at least some regions where brittle intermetallic phases were present and cracks were observed in these regions. Even the titanium to aluminium weld - which was sound in the aluminium-rich region - contained a few small micro-cracks in the small root area where high dilution with titanium had created brittle intermetallic phases.

References

1. Klages, K; Ruettimann, C.; and Olowinsky, A.M: Laser Beam Micro Welding of Dissimilar Metals; Proc of ICALEO 2003, Laser Institute of America, Jacksonville

2. Naeem, M; “Microjoining of Dissimilar Metals with Pulsed Nd: YAG Laser, Conference Proceeding; PICALEO 2006, Melbourne, Australia, March, 2006

3. Naeem, M; “Microwelding performance comparison between a low power (125W) pulsed Nd: YAG laser and a low power (100-200W) single mode fiber laser; Conference Proceeding PICALEO 2008, Beijing, China; April 2008

4. Dausinger F, Benefit of enhanced focusability of new YAG-Lasers, in Proceedings of the EALA, (2002) Bad Nauheim/Frankfurt, Germany